Iranian Journal of Science and Technology, Transactions of Civil Engineering
https://doi.org/10.1007/s40996-022-00872-3

RESEARCH PAPER

The Effects of MTMD and HBI on the Performance of a Benchmark Building Against Near-Field Earthquakes Using Fuzzy Logic

Farzaneh Hadizadeh[1] · **Hashem Shariatmadar**[1] · **Fatemeh Akhlaghi Amiri**[1]

Received: 14 August 2021 / Accepted: 4 April 2022

Abstract
Different techniques are used to decrease structural responses under earthquakes. Base isolation system is a passive technique which reduces relative displacement and acceleration of the structure, simultaneously. However, it sometimes increases the absolute displacement. Using active control force in the isolated system is an effective method to overcome this problem. In this paper, the performance of an 8-story steel framed benchmark structure with base isolation is improved using a combination of multi-tuned mass damper (MTMD) and an active control force at the isolation level. The effects of proposed method in minimizing the response of the structure under four near-field ground motions are investigated. The control force is determined using the Fuzzy Type-1 algorithm. The MTMD consists of two TMDs, which are placed on the first floor and on the roof. In addition, the effects of pulse-like shape in near-field earthquakes on response of controlled structure are examined. Based on the results obtained from the time history response, it is revealed that MTMD reduces relative displacement and absolute acceleration in two directions (x, y) up to a maximum value of 66% and 47%, respectively. The hybrid base isolation controller reduces absolute displacement by a maximum of 33%. Based on the results, it is possible to reduce the twisting in the irregular structure by the placement of actuators in the four corners of the architectural plan.

Keywords Structural control · Multi-tuned mass damper (MTMD) · Hybrid base isolation (HBI) · Fuzzy type 1 · Near-field earthquake · Response reduction

1 Introduction

During an earthquake, a significant portion of input energy is dissipated when the structure entry into the non-linear phase. Additionally, flexural plastic hinges are formed, resulting in postponing the entrance of other members to the non-linear stage (Salimbahrami and Naghipour 2021). During a near-field ground motions, energy is transferred to structures in a short time; subsequently, the structures receive the force suddenly, it sounds like a shock (Taniguchi et al. 2008). Instead of developing non-linear behavior and formation of plastic hinges over the height of the structure, the energy of the earthquake is absorbed by the first few plastic joints, and the moment redistribution does not occur all over the beam-column connections.

The dynamic response of the structures due to the seismic loads can be reduced by passive, active, semi-active or hybrid control systems. Numerous research has been conducted using of different controllers (Golmoghany et al. 2021; Mohebbi and Dadkhah 2021). A tuned mass damper (TMD) is one of the most widely used and accepted systems for the vibration control of structures subjected to earthquake loads (Kim 2016), first applied by Frahm (1911) to reduce the vibration in ships (Patten et al. 1996). Passive mass dampers alone may not dissipate energy quickly to prevent serious damage to the structures. Meantime, active control systems are able to adapt to different loading conditions, such as the pulse-type loading, and to control different modes of vibration (Yang and Agrawal 2002). Although TMDs effectively suppress vibrations, they are rarely used under near-field ground motion (Ozbulut et al. 2011). In this regard, there is a wide range of researches showing the performance of TMD against different earthquakes (Salvi et al.

✉ Hashem Shariatmadar
shariatmadar@um.ac.ir

Farzaneh Hadizadeh
eng.hadizadeh@alumni.um.ac.ir

Fatemeh Akhlaghi Amiri
Amiri1991@gmail.com

[1] Department of Civil Engineering, Ferdowsi University of Mashhad, Mashhad, Iran

Published online: 08 May 2022

2018; Quaranta et al. 2016; Etedali et al. 2019; Alizadeh and Lavassani 2021).

Another structural control system is base isolation (BI) that is mounted on the base level. It absorbs the maximum energy arising from the lateral loads by deforming, and therefore, it prevents transferring the total energy to the structure (Matta 2011).

Since the seismic behavior of the structures and control systems is complicated, a control method is needed to consider all complexities easily (Soong and Spencer 2000). Different lgorithms are used to generate active control force, among which the fuzzy system is recommended for this purpose (Ahlawat and Ramaswamy 2001; Pourzeynali et al. 2007; Guclu and Yazici 2008). It tolerates the uncertainties of the input data (Shariatmadar and Razavi 2014). It has the ability to handle the non-linear behavior of the structure caused by large displacements, material non-linearity and damage (Li et al. 2011a, b). Fuzzy also can be adaptive by modifying its rules or membership functions (Faravelli and Yao 1996).

In order to enhance the performance of base-isolated structures against near-field excitations, passive, active and semi-active control devices have been proposed (Ozbulut et al. 2011).

So far, numerous researches have been done on hybrid isolation (Dicleli 2007; Jung et al. 2007). Some scientists have investigated the response of seismically isolated structures and its deformation (Tsiavos et al. 2020). The application of the base isolation with a tuned-mass-damper (TMD) located at basement, below the isolation floor, is studied for improving the seismic performance of the building (De Domenico and Ricciardi 2018a, b). De Domenico and Ricciardi (2018a, b) have stated that the combination of base-isolation system and TMD shows an excellent level of vibration reduction in compared with the conventional base-isolation scheme, in terms of displacement of the base-isolation system and also the response of the isolated superstructure.

In another research, a resilient base-isolated building with a large mass-ratio TMD is introduced for earthquake loads in which the large mass-ratio TMD is located at basement showing robust for both pulse-type ground motions and long-period ground motions (Hashimoto et al. 2015).

Subramaniam et al. (1996) assessed the performance of the fuzzy algorithms in hybrid structural control systems. The fuzzy controller used feedback from the base acceleration or the force at the interface to produce control forces. The results demonstrated that fuzzy logic could be utilized for non-linear problems. Lin et al. (2007) performed several large-scale tests on a mass equipped with a base isolation system that included high damping rubber bearings and magneto-rheological (MR) damper under near-fault and far-fault earthquakes. The fuzzy controller used the feedback of the displacement, velocity and the acceleration of the structure. They compared the results of different types of passive and semi-active control strategies with each other. Shook et al. (2008) proposed a hybrid isolated system consisting of elastomeric and pendulum bearings, shape memory alloy (SMA) and MR dampers, each of which was designed for a unique task to reduce seismic responses. The SMA and MR dampers were modeled by the neuro-fuzzy system. The results illustrated that the model reduced base drifts by 18% .Mehrparvar et al. (2011) evaluated the function of active control systems in terms of reducing the responses of base-isolated structures under the near-fault ground motions. The design of the mentioned hybrid system was optimized to fulfill different desired purposes. In some cases, the equivalent passive system was introduced which had similar responses to the hybrid control system.

Suresh et al. (2012) studied a non-linear parametric controller to control base-isolated benchmark structure under near-fault ground motions. The non-linear control laws were estimated through a nonlinearly parameterized neural network, without any explicit training. The investigation indicated that the controller could reduce the response for a wide range of near-fault ground motions without increasing the superstructure response.

Giuseppe Oliveto et al. (2014) introduced a constrained optimization procedure for the dynamic analysis of the hybrid base isolation system against earthquake stimulation. They showed how to use one-dimensional analysis to predict a two-dimensional response. Mohebbi et al. (2015) studied the optimal design of hybrid low damping base isolation and MR damper. Optimization of the active isolator system minimized the maximum base drift using a genetic algorithm. In addition, it limited the maximum acceleration of the structure. The H2/LQG control algorithm was applied to determine the MR damper voltage. For numerical analysis, a 3-story structure with a hybrid isolator and MR damper was designed under Elcentro earthquake. Results proved the effectiveness of the optimal control system in controlling the maximum base drift of the isolators. Also, adding MR damper to the low damping isolator improved its performance, so it worked better than the high damping system.

Gazi and Alhan (2018) analyzed the failure probability of a nonlinear base-isolated system for a three-dimensional building model by Monte Carlo simulations. Alhan and Ozgur (2015) investigated the precision of an equivalent linear modeling for numerous different isolation systems. They performed numerical tests on a three-dimensional isolated building and found the accuracy of the peak structural response estimation.

The majority of the research has focused on structural response of structures equipped with only TMD or base isolation with much less attention paid to the effects of the combination of MTMD and BI especially when control force

are used. This research investigates the performance of such a system under some near-field earthquakes with considering the effects of pulse shape earthquake on the responses. In addition, the passive systems could not alone dissipate the energy of the near-field ground motions, immediately. On the other hand, the active devices are generally able to control the seismic response of the structure for a wide range of dynamic loading. Therefore, in this research, it is attempted to improve the seismic performance of structure subjected to near-field ground motions using a combination of hybrid base isolation and MTMD system.

2 Structural Modeling

In this research, the performance of the structure is compared in three cases including; base-isolated structure (BI), base-isolated structure with MTMD (BI + MTMD) and hybrid base-isolated structure with MTMD (HBI + MTMD). Choosing the installation location of TMD is an important factor to consider for evaluation of structural response (Lee et al. 2021). In this study, there is one TMD on roof and another on the first floor. The benchmark structure is a three-dimensional, eight-story, steel braced framed building which has base isolation system. The base isolation system consists of 61 non-linear isolator bearings (Friction Pendulum or LRB) and 31 linear elastomeric bearings (shown in Fig. 1). The total weight of the structure is 202,000 KN. It is assumed that the foundation and floor slabs are rigid in plane and have three degrees of freedom at their center of mass, and the superstructure has 24 degrees of freedom (24DOF) (Nagarajaiah and Narasimhan 2006). In addition, two TMDs (on roof and base floor) and the isolator (on base level) used in the structure have three DOF each, so the whole structure has 33 DOF.

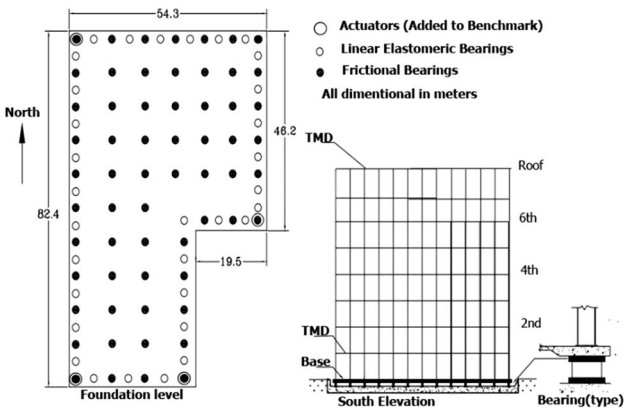

Fig. 1 Location of the control devices (actuators and isolators)

Four near-field earthquakes are considered for evaluation purposes. The earthquakes used in this study are Newhall (1994 Northridge Earthquake, Newhall county, Fault-Normal 360 and Fault-Parallel 90), El Centro (1994 Northridge Earthquake, El Centro record, Fault-Normal and Fault-Parallel), Rinaldi (1994 Northridge Earthquake, Rinaldi station, Fault-Normal 228 degrees and Fault-Parallel 318 degrees), Kobe (1995, JMA station, East–West and North–South components) (Nagarajaiah and Narasimhan 2006).

In addition, the control force is applied by actuators at isolator's level to improve the isolation performance and reduce the structural absolute displacement.

The superstructure is modeled as a three-dimensional linear elastic system with lateral-torsional behavior, and the nonlinearity is just assigned to the isolators (Nagarajaiah and Narasimhan 2006). Torsion in structural frames is one of the main reasons of damage to structures against ground motions (Oh et al. 2021). This structure is modeled and programmed by MATLAB and using the equations of structure's motion. Each non-linear isolation bearing modeled explicitly using discrete biaxial Bouc–Wen model (Nagarajaiah and Narasimhan 2006). Each TMD has 3 degrees of freedom at the center of mass and its mass, stiffness and damping parameters are added in the TMD level. The superstructure and TMDs are modeled together as a structure on the base isolation.

The equation of motion for the elastic superstructure is shown in Eq. (1):

$$M_{n\times n}\ddot{U}_{n\times 1}+C_{n\times n}\dot{U}_{n\times 1}+K_{n\times n}U_{n\times 1}=-M_{n\times n}R_{n\times 3}\left(\ddot{U}_g+\ddot{U}_b\right)_{3\times 1} \tag{1}$$

where n is three times the number of floors and TMDs, M is the superstructure and TMDs mass matrix, C is the superstructure and TMDs damping matrix in the fixed base case, K is the superstructure and TMDs stiffness matrix in the fixed base case, and R is the matrix of earthquake influence coefficients. In this equation, $\ddot{U}$, $\dot{U}$ and U represent the floor acceleration, velocity and displacement vectors relative to the base, $\ddot{U}_b$ is the vector of base acceleration relative to the ground, and $\ddot{U}_g$ is the vector of ground acceleration.

The equation of motion for base of structure (Nagarajaiah and Narasimhan 2006) is presented in Eq. (2):

$$\begin{aligned}&R_{3\times n}M_{n\times n}\left[(\measuredangle)_{n\times 1}+R_{n\times 3}\left(\measuredangle_g+\measuredangle_b\right)_{3\times 1}\right]_{n\times 1}\\&+M_{b_{3\times 3}}\left(\measuredangle_g+\measuredangle_b\right)_{3\times 1}+C_{b_{3\times 3}}\dot{U}_{b_{3\times 1}}+K_{b_{3\times 3}}U_{b_{3\times 1}}+f_{3\times 1}=0\end{aligned} \tag{2}$$

in which, M_b is the diagonal mass matrix of the rigid base, C_b is the viscous damping matrix of elastic isolation elements, K_b is the stiffness matrix of elastic isolation elements, and f is the vector of isolators forces.

This equation is solved using unconditionally stable Newmark's constant-average acceleration method (Nagarajaiah and Narasimhan 2006).

The damping ratio of the TMDs is considered 5% in all cases. The optimization formulas (3) and (4) have been used to obtain the TMD's frequency. In this equation, α_{opt} is the optimal frequency ratio for the TMD, μ is the percentage of the TMD's mass to the structure's mass, and α is the ratio of the TMD's frequency to the structure's frequency (Connor 2003).

$$\alpha_{\text{opt}} = \frac{\left(1 - \frac{\mu}{2}\right)^{1/2}}{1 + \mu} \tag{3}$$

$$w_d = \alpha w_s \tag{4}$$

The actuators, which apply active forces to isolators, are placed at the four corners of the structure plan, shown in Fig. 1. The mass ratio of each TMD for each earthquake is shown in Table 1. After having tested several mass ratios for TMDs and different locations for actuators, those which reduced the absolute displacement are chosen. Although the earthquakes have uncertainty and the mass ratio of TMD cannot be various in different earthquakes, this research attempts to illustrate the maximum reduction of structural response by selecting the optimum mass ratio of TMD for each earthquake.

3 Fuzzy Logic Controller (FLC)

The fuzzy set theory allows objects to have any degree of membership (between 0 and 100%) within a set (Symans and Kelly 1999). Fuzzy logic enables the use of linguistic directions as a basis for control, generally very capable for handling systems. The most widely used fuzzy control inference Ri is the "if–then" rule, which can be written as follows when two input data are used (Ahlawat and Ramaswamy 2001):

Ri: if × 1 = Ai, and × 2 = Bi then y = Ci.

The basic structure of a typical FLC is illustrated in Fig. 2, in which the components are defined as follows.

Table 1 Mass ratio of TMD

Earthquakes	μx (%)	μy (%)
Newhal	4	6
Elcentro	5	2
Rinaldi	5	1
Kobe	5	1

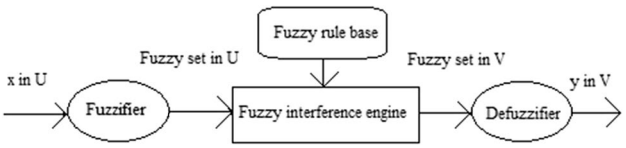

Fig. 2 FLC components

- Fuzzifier: The measured inputs in the control process, which may be in the form of crisp values, would be converted into fuzzy linguistic values using fuzzy reasoning mechanism.
- Fuzzy rules: This is a collection of the expert control rules needed to achieve the control goal.
- Fuzzy interference engine: This unit is the fuzzy reasoning mechanism, which performs various fuzzy logic operations to infer the control action for a given fuzzy input.
- Defuzzifier: The inferred fuzzy control action is converted into the required crisp control value in this unit.

The design of a fuzzy controller involves decisions about a number of important design parameters that should be determined before the actual control starts.

Some characteristics of FLC appealing to control engineers are their effectiveness and ease in handling structural nonlinearities, uncertainties and heuristic knowledge. Added to the niceties present in a fuzzy system, a fuzzy control applied to structural system can handle the hysteretic behavior of the structure under earthquake (Dyke et al. 1996).

All the rules in this paper are written using Mamdani method to apply to fuzzification, and the centroid method is used in defuzzification.

The HBI controller force is obtained by type 1 fuzzy algorithm. In this research, the fuzzy controller has two input variables which are displacement and velocity of four base corners. Each of them has seven triangular membership functions (MFs), as shown in Fig. 3.

The control force is the output variable, and it has seven triangular membership functions, as presented in Fig. 4.

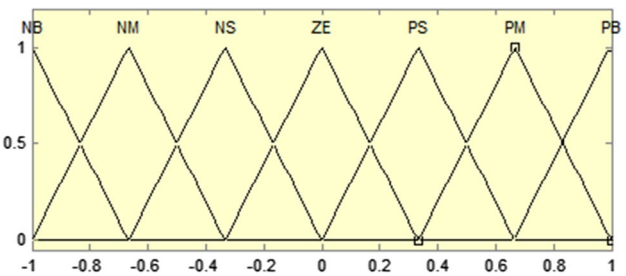

Fig. 3 MFs of input variables

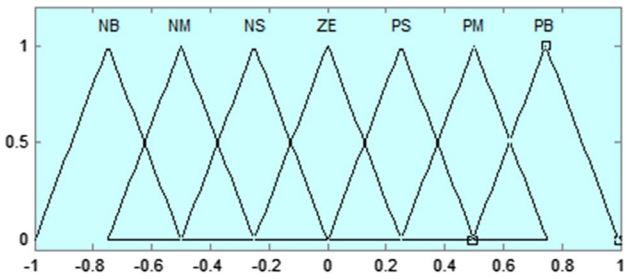

Fig. 4 MFs of output variables

Table 2 Concept of fuzzy variables

Membership function	Variable	Definition
Input and output	P	Positive
	Z	Zero
	N	Negative
	PVB	Positive very big
	PB	Positive big
	PM	Positive medium
	PS	Positive small
	PVS	Positive very small
	Z	Zero
	NVS	Negative very small
	NS	Negative small
	NM	Negative medium
	NB	Negative big
	NVB	Negative very big

The concept of input and output variables is given in Table 2.

The fuzzy rule-bases are formed with the help of an expert's knowledge and input and output variables. The more detailed rules are written, and the more accurate active control force actuator produces and applies to the structure. Thereupon, the structure response decreases over time.

In this research, three fuzzy rule bases were used to control the response of the structure. One of them, which appropriately reduced the structure response at base level, was chosen as the rule base of the HBI controller.

A trial and error approach with triangular membership functions has been used to achieve a good controller performance.

These rule bases have 9, 25 and 49 rules, as presented in Tables 3, 4 and 5, respectively.

The base-level response of a structure with HBI and MTMD under the selective earthquake, Rinaldi, is presented in two directions X and Y with aforesaid rule bases in Table 6.

In this research, the aim of using the control force is reduction of displacement at the base level. According to these results, the one containing 49 rules estimated optimal control force and reduced the structure response in base level by 18% on average, while using 9 and 25 rules decreased by 13% and 2% in average, respectively. So this rule base is selected for analyzing the response of the benchmark structure.

Table 3 Fuzzy rule base with 9 rules

Velocity	Displacement		
	N	Z	P
N	PB	PM	PS
Z	PS	Z	NS
P	NS	NM	NB

Table 4 Fuzzy rule base with 25 rules

Velocity	Displacement				
	NB	NS	Z	PS	PB
NB	PVB	PB	PM	PS	PVS
NS	PB	PM	PS	PVS	Z
Z	PB	PS	Z	NS	NB
PS	Z	NVS	NS	NM	NB
PB	NVS	NS	NM	NB	NVB

4 Double-Pulse Ground Motion

Pulse-like ground motions, which are mainly seen in near-fault ground motions, cause severe damages on structures. In this part, a simple and effective method named zero velocity point method (ZVPM) is introduced to identify pulse-like ground motions numerically (Zhao et al. 2016). The amount of the energy for the detected velocity pulse to the energy of the original ground motion is used to develop the identification criteria.

Pulse-like ground motions are classified into two classes: single-pulse-like and multi-pulse-like. Multi-pulse-like is divided into double-pulse-like, three-pulse-like, and four-pulse-like. Energy method is adopted to formulate the identification criterion for each type of pulse-like ground motion.

The criteria to identify multi-pulse-like ground motions are elucidated as follows (Zhao et al. 2016).

1. Confirming that the given ground motion is not significant-single-pulse-like ground motion.
2. In the selected vibration intervals, the period and energy ratio must not be less than 0.5 s and 0.2, respectively.
3. If the number of the satisfied vibration intervals is less than 2, then the ground motion is not multi-pulse-like ground motion.

Table 5 Fuzzy rule base with 49 rules (Li et al. 2011a, b)

Velocity	Displacement						
	NB	NM	NS	Z	PS	PM	PB
NB	PB	PB	PM	PM	PS	PS	Z
NM	PB	PM	PM	PS	PS	Z	NS
NS	PM	PM	PS	PS	Z	NS	NS
Z	PM	PS	PS	Z	NS	NS	NM
PS	PS	PS	Z	NS	NS	NM	NM
PM	PS	Z	NS	NS	NM	NM	NB
PB	Z	NS	NS	NM	NM	NB	NB

Table 6 Displacement response of the base level

Direction	Displacement of isolated structure(m)	Displacement of structure with HBI and TMD		
		9rules	25rules	49rules
X	0.29	0.23	0.30	0.20
Y	0.41	0.39	0.38	0.39

4. If the number of the satisfied vibration interval is 2, and the summation of the energy ratio for the two satisfied vibration intervals is not less than 0.6, then the ground motion is a double-pulse-like ground motion.

The energy of the ground motion can be computed by Eq. (5) (Zhao et al. 2016):

$$E = \Delta t \sum_{i=1}^{N} V_i^2 \tag{5}$$

in which V_i is velocity, Δt is the time interval of the ground motion, and N is the number of discrete points of the ground motion. The ground motion energy in the interval of I_k can be defined by Eq. (6).

$$E_k = \Delta t \sum_{i=1}^{N_k} V_i^2 \tag{6}$$

In this article, t_i ($i = 1, 2, 3, \ldots$) is defined as the ith point at which the velocity model value equals zero, and I_k (k = 1, 2, 3, …) is defined as the kth vibration interval (the length to complete a cycle of vibration). Therefore, $t = 0$ is the first point where velocity value equals zero. Also, I_k is defined by Eq. (7).

$$I_k = \left[t_{2k-1}, t_{2k+1}\right], \ (k = 1, 2, 3, \ldots). \tag{7}$$

Relative energy ER_k is calculated by Eq. (8).

$$\mathrm{ER}_k = \frac{E_k}{E} \tag{8}$$

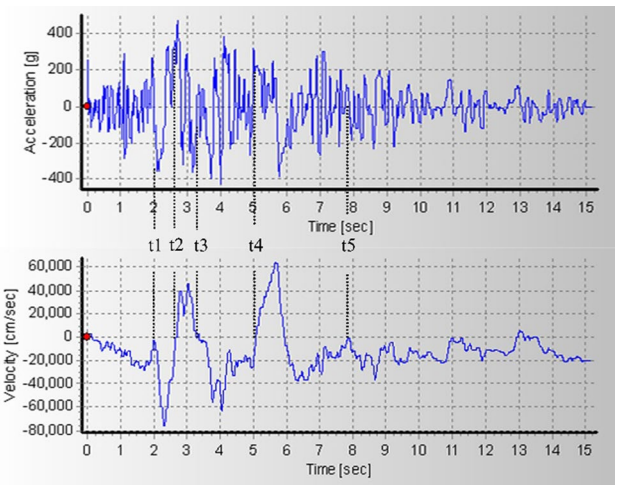

Fig. 5 Zero velocity point method to detect the vibration intervals of Rinaldi earthquake FP

The acceleration and velocity time histories of the Rinaldi earthquake FP are shown in Fig. 5.

According to Eq. 8, the energy of the mentioned ground motion is calculated:

ER1 = 0.245 [t3 , t5]

ER2 = 0.0362 [t1 , t3]

Therefore, energy ratio is equal to 0.61, and the Rinaldi earthquake FP is considered as a double-pulse-like ground motion.

When this method is applied to all near-fault ground motions, it is revealed that Rinaldi and Kobe earthquakes FP are double-pulse ground motion.

5 Results Evaluation

The result of structural responses for different controllers subjected to near-field ground motions are evaluated and compared in this section.

5.1 Absolute and Relative Displacement Responses

The peak absolute displacement of the controlled structure under the Rinaldi and Newhall earthquakes in X- and Y-directions is illustrated in Figs. 6 and 7, respectively. It is clear that although MTMD has no significant effect on the reduction of absolute displacement response due to twisting in the irregular structure or pulse-shape of near-field ground motions, the combination of MTMD and HBI has reduced the peak absolute displacement response maximum by approximately 33% and 10% under the Rinaldi, and 21% and 10% under the Newhall earthquake in the directions of X and Y, sequentially.

The RMS absolute displacement of the controlled structures under the Kobe and Elcentro earthquakes is demonstrated in Figs. 8 and 9, respectively. The RMS response for structure equipped with MTMD and HBI decreased by 23% and 16% in the Kobe, and 11% and 10% under Elcentro earthquake in the X- and Y- directions, sequentially. It is stated that using the proposed hybrid system (HBI + MTMD) can improve the weakness of MTMD

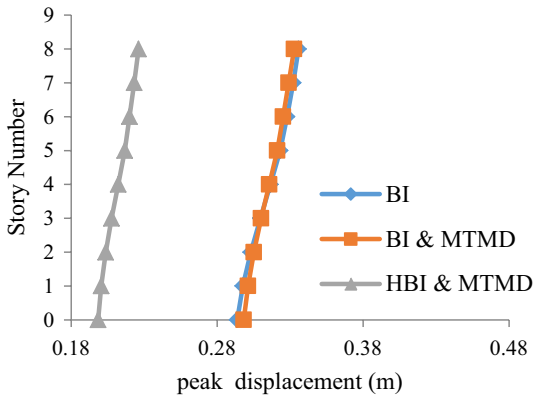

(a) X-direction

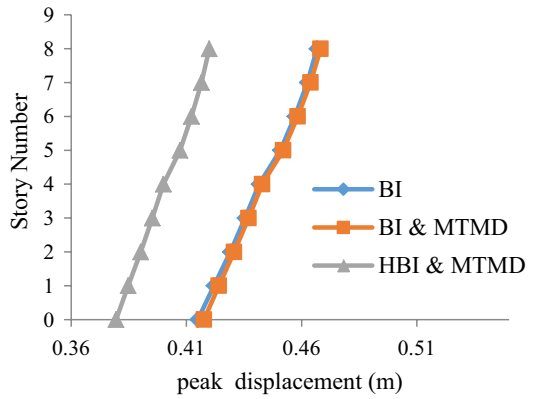

(b) Y-direction

Fig. 6 Peak absolute displacement of structure under the Rinaldi earthquake

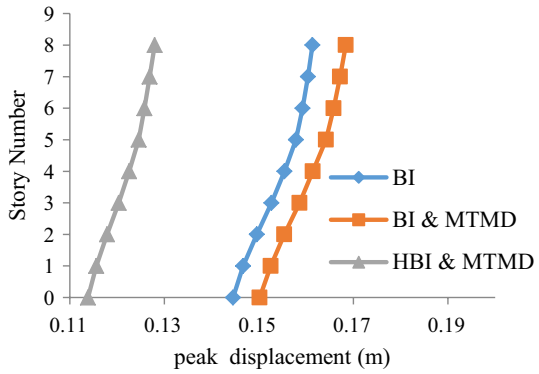

(a) X-direction

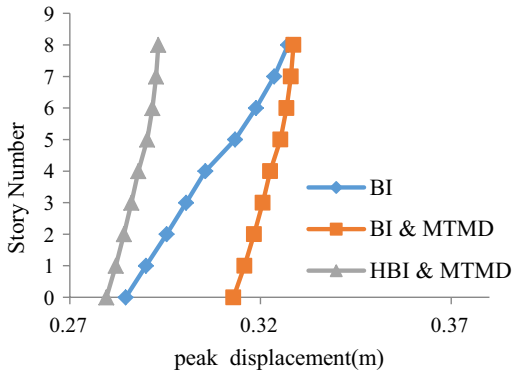

(b) Y-direction

Fig. 7 Peak absolute displacement of structure under the Newhall earthquake

to decrease the absolute displacement of structure under near-field ground motions.

The peak relative displacement of the structure under the Rinaldi and Newhall earthquakes is shown in Figs. 10 and 11. As can be noticed, the MTMD controller reduces the relative displacement response of the floors.

The relative displacement is changed for each floor in different directions for various earthquakes due to the difference in the earthquakes acceleration records and the torsion of the irregular structure. The maximum reduction of peak relative displacement in the base-isolated structure with MTMD under the Rinaldi and Newhall earthquakes in the X-direction is 23% and 37%, and in the Y-direction is 64% and 8% sequentially.

Figures 12 and 13 illustrate the RMS relative displacement of the structure under the Kobe and Elcentro earthquakes. The RMS relative displacement of this structure with adding MTMD is reduced by 26% and 9% under the Kobe and 30% and 8% under Elcentro earthquake in the X- and Y- directions sequentially.

The addition of HBI does not have a significant effect on reducing the relative displacement of the structure.

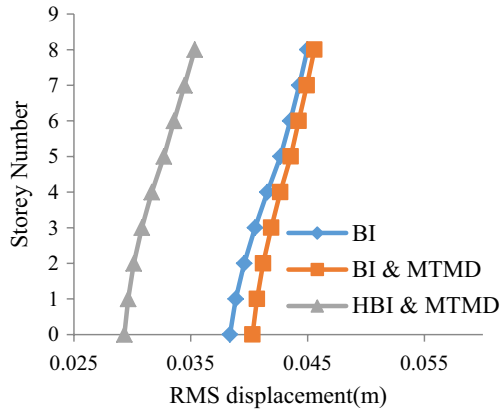

(a) X-direction

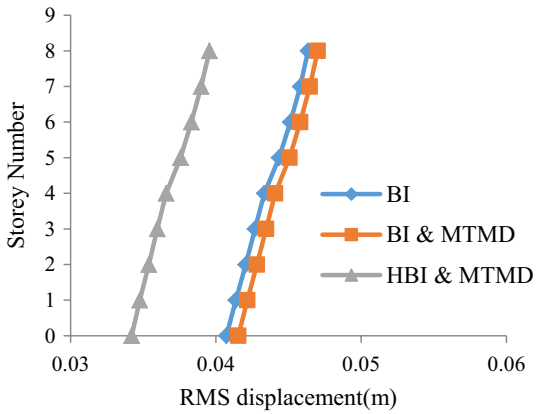

(b) Y-direction

Fig. 8 RMS absolute displacement of the structure under the Kobe earthquake

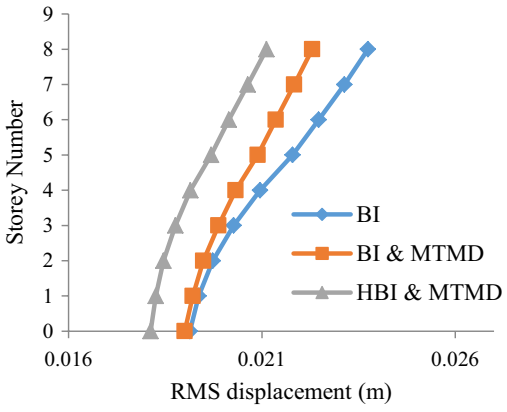

(a) X-direction

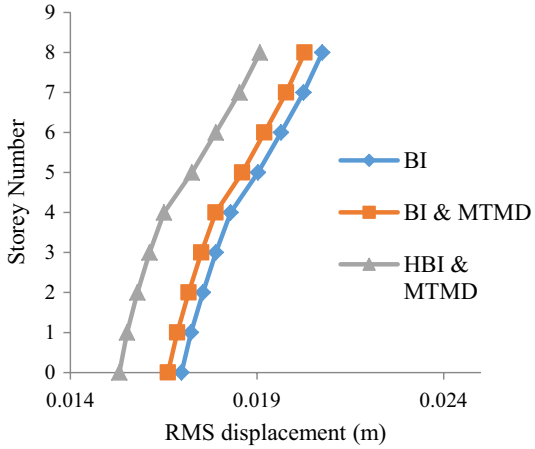

(b) Y-direction

Fig. 9 RMS absolute displacement of structure under the Elcentro earthquake

In all cases, maximum drifts have occurred in the 5th story. It can be inferred that TMD on the first floor and roof reduces drift in the same floors well, but this effect is approximately eliminated in far floors like 5th.

5.2 Comparison of the Controller Performance

The maximum reduction percentage of the peak and RMS absolute displacement for the structure equipped with MTMD and HBI controller under four near-field ground motions is presented in Figs. 14 and 15, respectively. As can be seen in Fig. 13, the combination of HBI and MTMD in all earthquakes has reduced the peak absolute displacement response in the best case by almost 33% and 21% in X- and Y-directions, respectively. The RMS absolute displacement varies between 11 and 32% in the X- direction, and 9% and 22% in the Y-direction (see Fig. 14). Adding only MTMD to base-isolated structure does not reduce the absolute displacement significantly.

Figures 16 and 17 compare the peak and RMS reduction percentage of relative displacement for the structure with MTMD and HBI. As can be shown in Fig. 16, the function of the controllers varies in different directions under each earthquake. The maximum reduction of peak relative displacement using MTMD controller is 38% in the X-direction under the Elcentro earthquake and 64% in the Y-direction under the Newhall earthquake. Also, the reduction of the RMS response shown in Fig. 17 is 34% in the X-direction under the Rinaldi earthquake and about 66% in the Y-direction under the Newhall earthquake. Using actuator added base-isolated structure equipped with MTMD does not have meaningful changes in the response.

The reduction percentage of peak and RMS absolute acceleration for the controlled structure is demonstrated in Figs. 18 and 19.

The MTMD causes the peak absolute acceleration of the structure to decline by 44% and 30% in the X- and Y-directions sequentially (see Fig. 18). Meanwhile, the RMS absolute acceleration of the base-isolated structure with MTMD shown in Fig. 19 decreases by 47% in the X-direction under

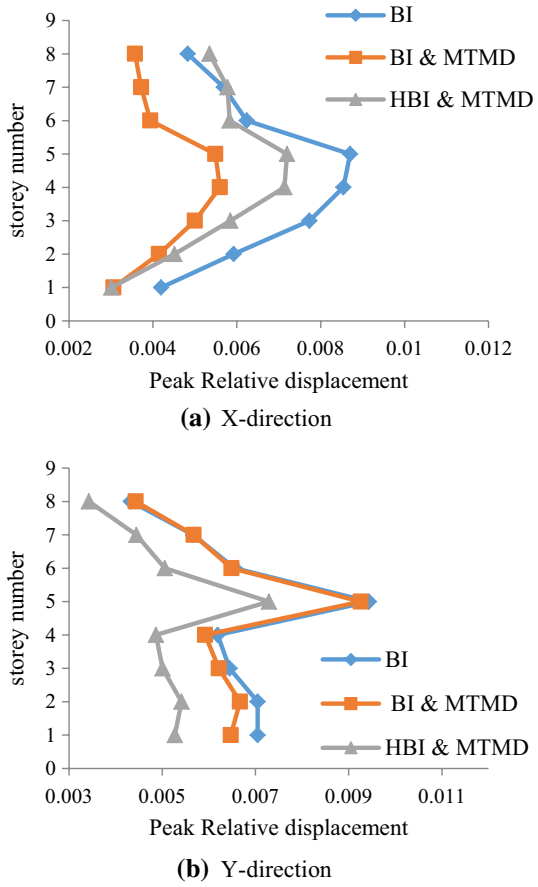

Fig. 10 Peak relative displacement of the structure under the Rinaldi earthquake

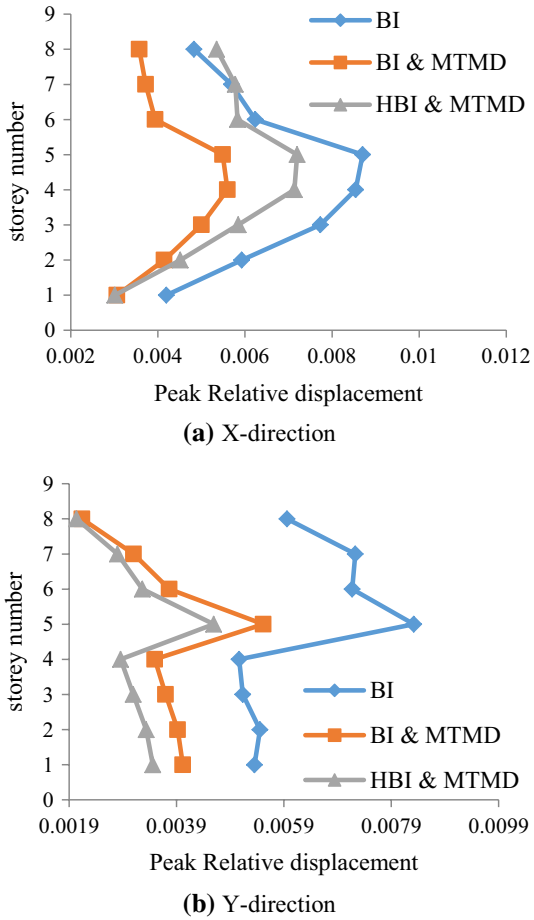

Fig. 11 Peak relative displacement of the structure under the Newhall earthquake

the Kobe earthquake and 44% in the Y-direction under the Newhall earthquake. As can be clearly noticed, the reduction of RMS absolute acceleration does not follow a regular trend.

6 Displacement Time History Response

The time history responses at the base in both X- and Y-directions are presented in Figs. 20, 21, 22 and 23 subjected to different earthquakes. The peak ground accelerations in earthquake records are generally smaller in fault-parallel direction compared to that for fault-perpendicular direction. Having lower induced forces in parallel direction to fault and assigning the same gains for the control force in both directions, resulting in more significant reduction of the response in X-direction compared to Y-direction. However, the first peak response in Y-direction is not reduced due to high value of acceleration in excitation records.

The displacement response in X-direction for Rinaldi earthquake has been reduced (Fig. 20a). The acceleration record of Rinaldi in fault-parallel direction has double pulse. Although the first pulse has less amount, it causes the TMDs start to act; in addition, due to first pulse response, the actuator receives the command to apply control force; consequently, the max peak displacement response (appeared later) has been decreased. However, there is only one pulse in Y-direction, which is not enough time for desirable performance (Fig. 20b).

The response in X-direction for Newhall earthquake has been decreased (Fig. 21a). The acceleration record for this earthquake in fault-parallel direction has several peaks. The first peaks lead TMDs to initiate to act and, in addition, sending command to actuator for applying control force; consequently, the other max peak displacement has also been decreased (Fig. 21a). Nevertheless, the record in Y-direction is single-pulse, which does not provide enough time for displacement reduction (Fig. 21b).

As the displacement time history for Kobe earthquake (Fig. 22) reveals, the pick response in two directions has been reduced. Kobe in X-direction is a double-pulse-shape ground excitation which causes the MTMD to operate and

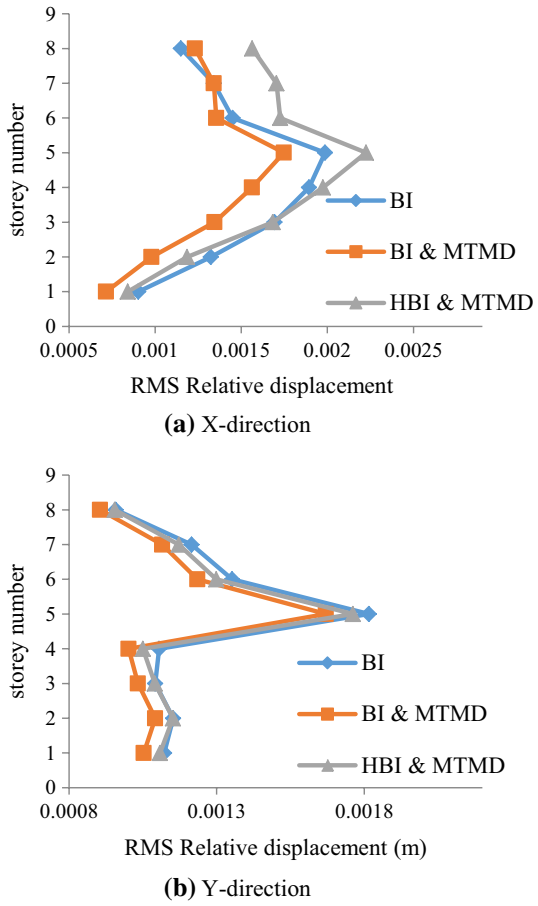

Fig. 12 RMS relative displacement of the structure under the Kobe earthquake

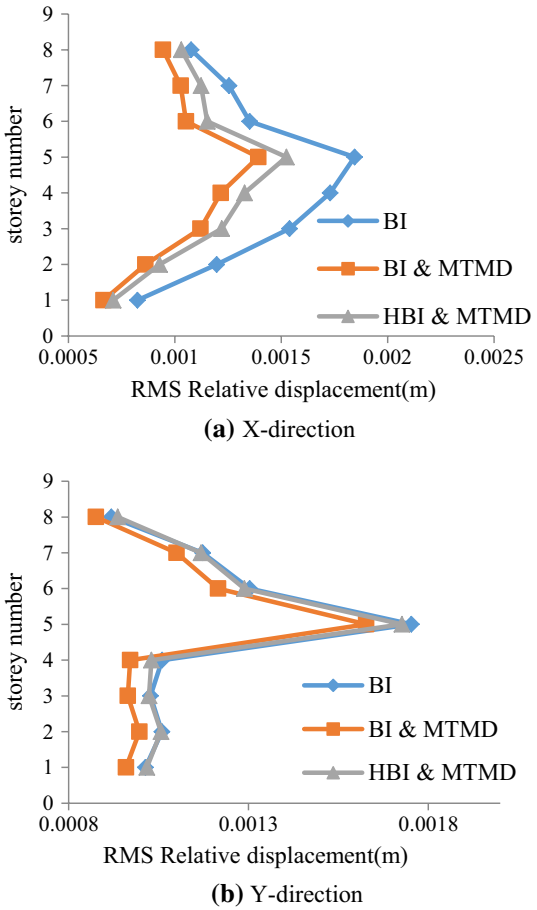

Fig. 13 RMS relative displacement of the structure under the Elcentro earthquake

active control force to be provided for effectual performance simultaneously.

Elcentro acceleration record has lots of peaks during the earthquake time (Nagarajaiah and Narasimhan 2006) which stimulates isolation system, so the actuators apply force continuously. Therefore, the maximum displacements in both X- and Y-directions have been reduced significantly (Fig. 23). However, due to pulse with very short time at the middle of earthquake acceleration time history (from 10 s up to 15 s), the structural response remains in one direction; thus, after reduction in maximum displacement, the other pick responses have not been reduced.

In general, the controller has reduced the response in both directions. However, the maximum response in Y- direction, which occurred at the first pick, has not been decreased when structure subjected to Newhall and Rinaldi. This phenomenon is due to single-pulse-shape earthquake and structural irregularity. On the other hand, maximum response in Y-direction in Kobe and Elcentro earthquakes is reduced using HBI.

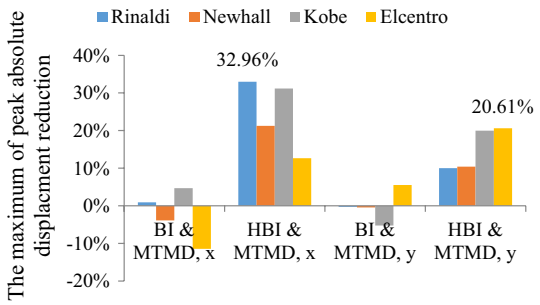

Fig. 14 Comparison of the peak absolute displacement maximum reduction for different controllers

7 Base Shear

The coefficient of base shear of the structure with different control strategies (BI, BI & MTMD, HBI & MTMD) under various earthquakes is compared in Fig. 24. The active force of HBI controller reduces base shear of the isolated

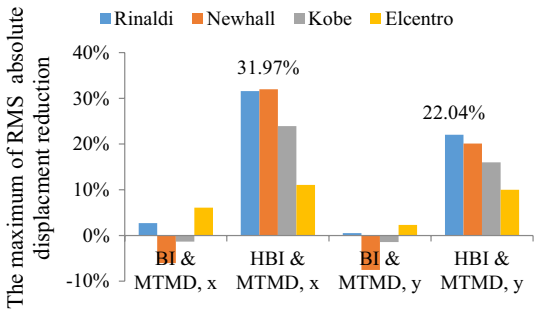

Fig. 15 Comparison of the RMS absolute displacement maximum reduction for different controllers

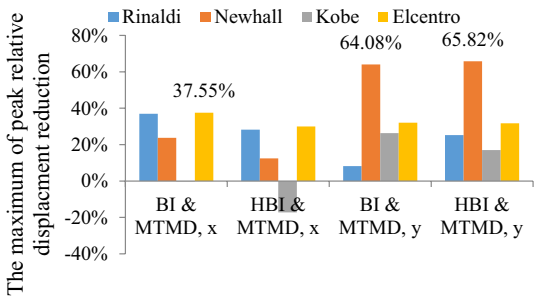

Fig. 16 Comparison of the peak relative displacement maximum reduction for different controllers

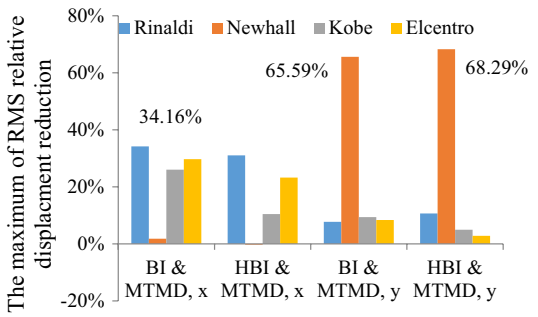

Fig. 17 Comparison of the RMS relative displacement maximum reduction for different controllers

structure about 10% for Newhall, Rinaldi and Kobe earthquakes. This indicates that fuzzy logic in active method can control the base shear of structure under very impulsive near-field earthquake. However, the active controller does not significantly reduce the base shear of structure subjected to the Elcentro earthquake. Nevertheless, using the MTMD to control the structure response slightly increases the base shear. This may be related to frequency content of near-fault earthquake, which is close to frequency of the equipped structure the MTMD.

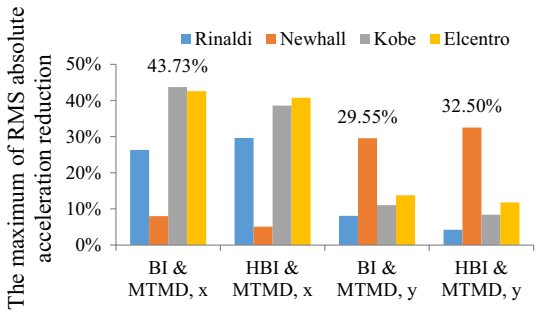

Fig. 18 Comparison of the peak absolute acceleration maximum reduction for different controllers

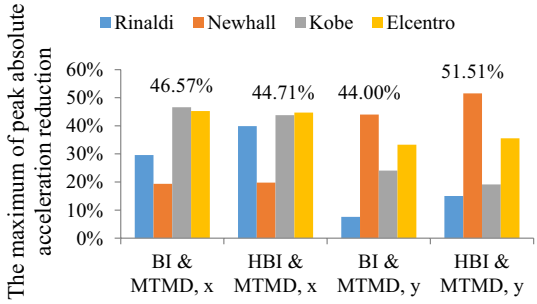

Fig. 19 Comparison of the RMS absolute acceleration maximum reduction for different controllers

8 Control Force

The maximum actuator force in eight devices and two directions is shown in Table 7. The amount of each actuator force is calculated between 3 and 7% of the base shear force to reduce the absolute displacement of the structure. In some cases, the actuator force is higher for earthquake with smaller peak ground acceleration, which is related to the type of earthquake. In most cases, the control force is determined based on the multi-pulse shape of the ground motion. Meanwhile, the variety in the control force for different locations of actuator is due to the torsional behavior of irregular structure. However, these control forces are close to the average of four devices.

The time history of the control force in the X- and Y-directions under the Kobe earthquake is shown in Fig. 25.

9 Conclusion

This structure is modeled in three dimensions. The structure is L-shape and irregular resulting in twisting and noticeable displacements. In addition, near field ground

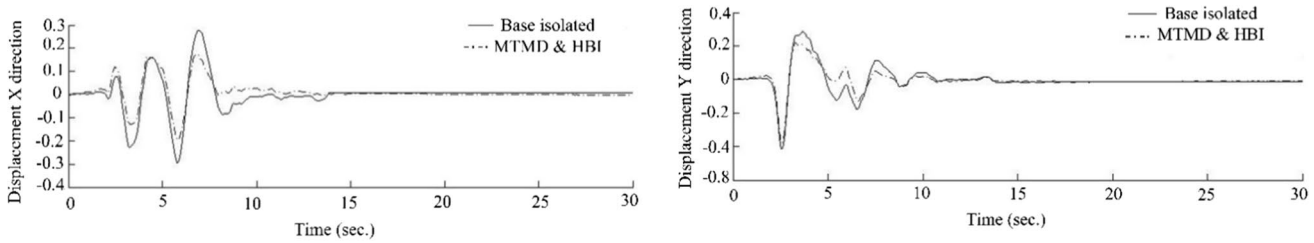

(a) X-direction **(b)** Y-direction

Fig. 20 The displacement of the center of mass in the base level under Rinaldi earthquake

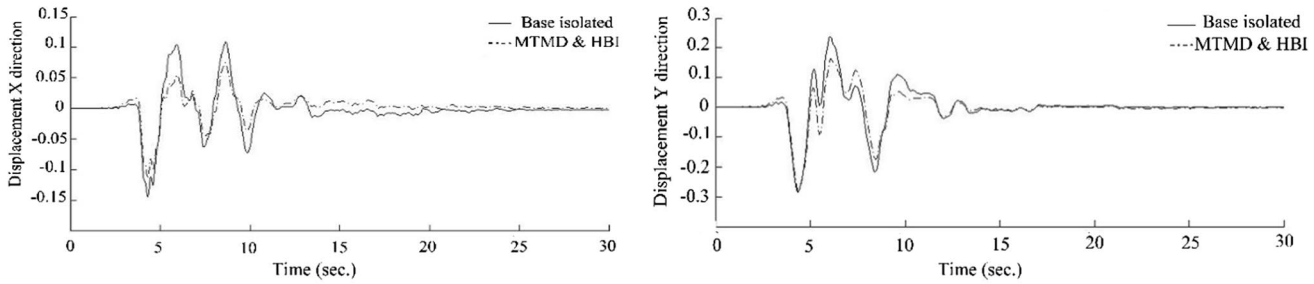

(a) X-direction **(b)** Y-direction

Fig. 21 The displacement of the center of mass in the base level under Newhall earthquake

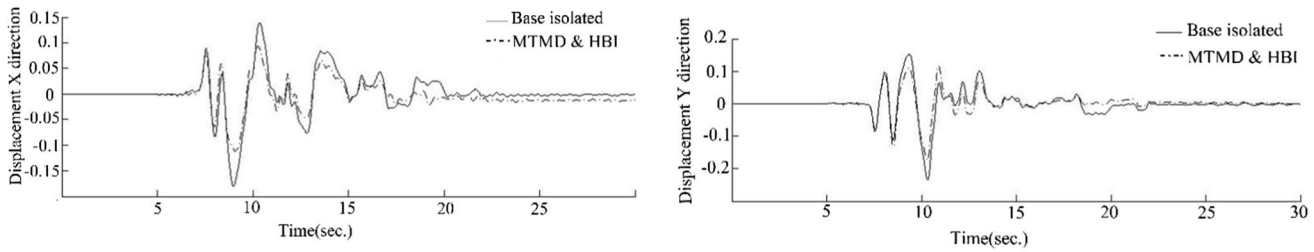

(a) X-direction **(b)** Y-direction

Fig. 22 The displacement of the center of mass in the base level under Kobe earthquake

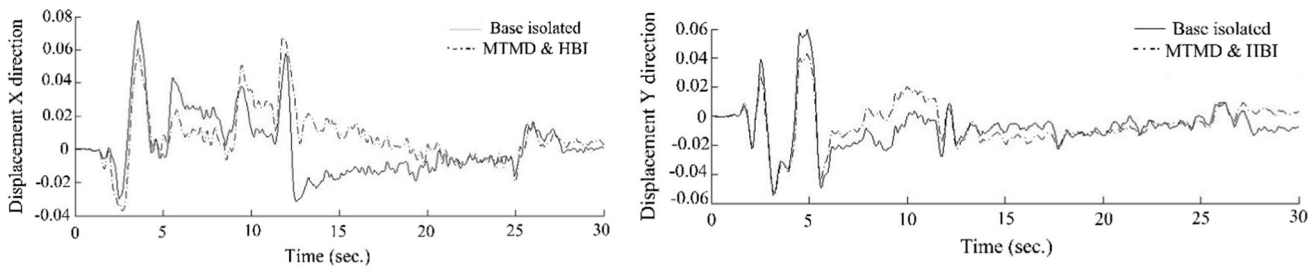

(a) X-direction **(b)** Y-direction

Fig. 23 The displacement of the center of mass in the base level under Elcentro earthquake

motions aggravate the circumstance and increase the response of structure. Using different controllers in structures is investigated. Research has shown that the absolute displacement in base isolation system leads damages especially in base level. Moreover, using a passive controller such as MTMD cannot operate quickly enough in

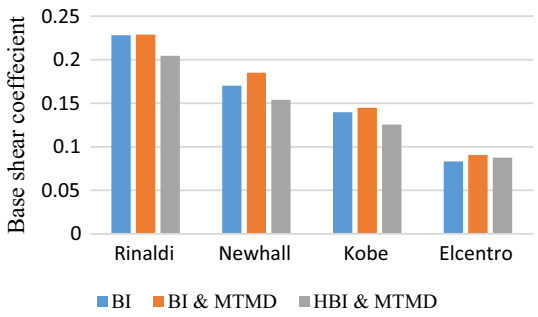

Fig. 24 Base shear of the structure with HBI and MTMD

Table 7 Actuators force (KN)

	Actuator number	Earthquake			
		Rinaldi	Newhall	Kobe	Elcentro
X direction	1	2732	2250	1673	1043
	2	2601	2250	1815	955
	3	2619	2234	1861	1115
	4	2719	2250	1734	1117
Y direction	5	2499	1980	1561	937
	6	2499	1725	1375	951
	7	2521	1811	1574	1026
	8	2496	1752	1395	1067

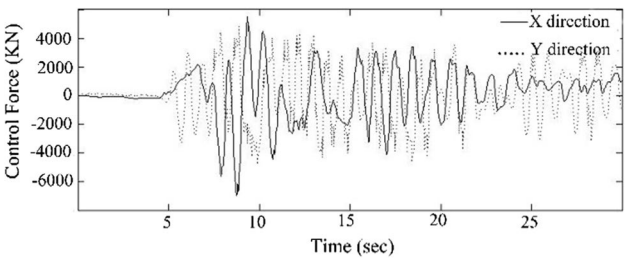

Fig. 25 Control forces of hybrid base isolation needed in Kobe earthquake

near-field earthquake. Meanwhile, twisting in an irregular structure sometimes leads increasing in response. In this article, it is attempted to assess the performance of controlled structure with combined MTMD and HBI against four near-field ground motions. The results of this study are elucidated as follows.

1. Using the rule base with more accurate and optimum fuzzy rules (49 compared to 9 and 25) in the hybrid base isolation system (HBI) decreases absolute displacement of base up to 18% on average.
2. Adding the MTMD to the isolated structure decreases the RMS relative displacement, in the best case, by up to 34% in the X-direction and 66% in the Y-direction. The reduction for maximum relative displacement is almost in the same range.
3. In the isolated structure with using MTMD, the absolute acceleration and its RMS are reduced in X-direction by 8–44% and 19–46%, respectively. Also, the absolute acceleration and its RMS are decreased in Y-direction by 8–30% and 8–44% sequentially for all near-field ground motions. Therefore, using MTMD to reduce the acceleration of structure under near-field ground motions is suitable.
4. The combination of MTMD and HBI reduces the RMS absolute displacement by 11–32% in the X-direction and 10–22% in the Y-direction for all earthquakes. Consequently, the using of this combination is recommended for the reduction of absolute displacement.
5. The maximum absolute displacement of the structure using MTMD and HBI in the best case decreases the response by 33% in the X-direction and 21% in the Y-direction subjected to Rinaldi earthquake.
6. Regarding to irregular structure, the placement of the actuators in the four corners of the architectural plan reduces the twisting.
7. Adding active control force (HBI) to the base-isolated structure reduces the structural base shear up to 10%.
8. For earthquakes with double-pulse-shape in their acceleration time history ground motion, the hybrid controller reduces the displacement responses.

References

Ahlawat AS, Ramaswamy A (2001) Multiobjective optimal structural vibration control using fuzzy logic control system. J Struct Eng 127(11):1330–1337

Alhan C, Ozgur M (2015) Seismic responses of base-isolated buildings: efficacy of equivalent linear modeling under near-fault earthquakes. Smart Struct Syst 15(6):1439–1461

Alizadeh H, Lavassani SHH (2021) Flutter control of long span suspension bridges in time domain using optimized TMD. Int J Steel Struct 21(2):731–742

Connor JJ (2003) Structural motion control. Pearson Education Inc, New York, p 220

De Domenico D, Ricciardi G (2018a) An enhanced base isolation system equipped with optimal tuned mass damper inerter (TMDI). Earthq Eng Struct Dynam 47(5):1169–1192

De Domenico D, Ricciardi G (2018b) Earthquake-resilient design of base isolated buildings with TMD at basement: application to a case study. Soil Dyn Earthq Eng 113:503–521

Dicleli M (2007) Supplemental elastic stiffness to reduce isolator displacements for seismic-isolated bridges in near-fault zones. Eng Struct 29(5):763–775

Dyke SJ, Spencer BF Jr, Sain MK, Carlson JD (1996) Modeling and control of magnetorheological dampers for seismic response reduction. Smart Mater Struct 5(5):565

Etedali S, Akbari M, Seifi M (2019) MOCS-based optimum design of TMD and FTMD for tall buildings under near-field earthquakes including SSI effects. Soil Dyn Earthq Eng 119:36–50

Faravelli L, Yao T (1996) Use of adaptive networks in fuzzy control of civil structures. Comput Aided Civ Infrastruct Eng 11(1):67–76

Frahm HUS (1911) Patent No. 989,958. U.S. Patent and Trademark Office 1911, Washington, DC

Gazi H, Alhan C (2018) Probabilistic sensitivity of base-isolated buildings to uncertainties. Smart Struct Syst 22(4):441–457

Golmoghany MZ, Zahrai SM (2021) Improving seismic behavior using a hybrid control system of friction damper and vertical shear panel in series. In: Structures, vol. 31. Elsevier, pp 369–379

Guclu R, Yazici H (2008) Vibration control of a structure with ATMD against earthquake using fuzzy logic controllers. J Sound Vib 318(1–2):36–49

Hashimoto T, Fujita K, Tsuji M, Takewaki I (2015) Innovative base-isolated building with large mass-ratio TMD at basement for greater earthquake resilience. Future Cities Environ 1(1):1–19

Jung HJ, Choi KM, Park KS, Cho SW (2007) Seismic protection of base isolated structures using smart passive control system. Smart Struct Syst 3(3):385–403

Kim HS (2016) Seismic response control of adjacent buildings coupled by semi-active shared TMD. Int J Steel Struct 16(2):647–656

Lee YR, Kim HS, Kang JW (2021) Seismic response control performance evaluation of tuned mass dampers for a retractable-roof spatial structure. Int J Steel Struct 21(1):213–224

Li J, Dackermann U, Xu YL, Samali B (2011a) Damage identification in civil engineering structures utilizing PCA-compressed residual frequency response functions and neural network ensembles. Struct Control Health Monit 18(2):207–226

Li L, Song G, Ou J (2011b) Hybrid active mass damper (AMD) vibration suppression of nonlinear high-rise structure using fuzzy logic control algorithm under earthquake excitations. Struct Control Health Monit 18(6):698–709

Lin PY, Roschke PN, Loh CH (2007) Hybrid base-isolation with magnetorheological damper and fuzzy control. Struct Control Health Monit off J Int Assoc Struct Control Monit Eur Assoc Control Struct 14(3):384–405

Matta E (2011) Performance of tuned mass dampers against near-field earthquakes. Struct Eng Mech Int J 39(5):621–642

Mehrparvar B, Khoshnoudian F (2011) Efficiency of active systems in controlling base-isolated buildings subjected to near-fault earthquakes. Struct Design Tall Spec Build 20(8):1019–1034

Mohebbi M, Dadkhah H (2021) An adaptive control algorithm for smart base isolation systems based on seismic early warning system. In: Structures, vol. 30. Elsevier, pp 638–646

Mohebbi M, Dadkhah H, Shakeri K (2015) Optimal hybrid base isolation and MR damper. Iran Univ Sci Technol 5(4):493–509

Nagarajaiah S, Narasimhan S (2006) Smart base-isolated benchmark building. Part II: phase I sample controllers for linear isolation systems. Struct Control Health Monit 13(2–3):589–604

Oh SH, Shin SH, Bagheri B (2021) Effect of torsion on seismic response of single-story structures: an energy-based design approach (EBD). Int J Steel Struct 21(3):820–835

Oliveto G, Oliveto ND, Athanasiou A (2014) Constrained optimization for 1-D dynamic and earthquake response analysis of hybrid base-isolation systems. Soil Dyn Earthq Eng 67:44–53

Ozbulut OE, Bitaraf M, Hurlebaus S (2011) Adaptive control of base-isolated structures against near-field earthquakes using variable friction dampers. Eng Struct 33(12):3143–3154

Patten WN, Sack RL, He Q (1996) Controlled semiactive hydraulic vibration absorber for bridges. J Struct Eng 122(2):187–192

Pourzeynali S, Lavasani HH, Modarayi AH (2007) Active control of high rise building structures using fuzzy logic and genetic algorithms. Eng Struct 29(3):346–357

Quaranta G, Mollaioli F, Monti G (2016) Effectiveness of design procedures for linear TMD installed on inelastic structures under pulse-like ground motion. Earthq Struct 10(1):239–260

Salimbahrami SR, Naghipour M (2021) Numerical study to evaluate the effect of ductile element in the seismic performance of steel frames with EBF. Int J Steel Struct 21(2):549–560

Salvi J, Rizzi E, Rustighi E, Ferguson NS (2018) Optimum tuning of passive tuned mass dampers for the mitigation of pulse-like responses. J Vib Acoust 140(6):061014

Shariatmadar H, Razavi HM (2014) Seismic control response of structures using an ATMD with fuzzy logic controller and PSO method. Struct Eng Mech 51(4):547–564

Shook DA, Roschke PN, Ozbulut OE (2008) Superelastic semi-active damping of a base-isolated structure. Struct Control Health Monit 15(5):746–768

Soong TT, Spencer BF (2000) Active, semi-active and hybrid control of structures. Bull N Z Soc Earthq Eng 33(3):387–402

Subramaniam RS, Reinhorn AM, Riley MA, Nagarajaiah S (1996) Hybrid control of structures using fuzzy logic. Comput Aided Civ Infrastruct Eng 11(1):1–17

Suresh S, Narasimhan S, Nagarajaiah S (2012) Direct adaptive neural controller for the active control of earthquake-excited nonlinear base-isolated buildings. Struct Control Health Monit 19(3):370–384

Symans MD, Kelly SW (1999) Fuzzy logic control of bridge structures using intelligent semi-active seismic isolation systems. Earthq Eng Struct Dyn 28(1):37–60

Taniguchi T, Der Kiureghian A, Melkumyan M (2008) Effect of tuned mass damper on displacement demand of base-isolated structures. Eng Struct 30(12):3478–3488

Tsiavos A, Haladij P, Sextos A, Alexander NA (2020) Analytical investigation of the effect of a deformable sliding layer on the dynamic response of seismically isolated structures. In: Structures, vol 27. Elsevier, pp 2426–2436

Yang JN, Agrawal AK (2002) Semi-active hybrid control systems for nonlinear buildings against near-field earthquakes. Eng Struct 24(3):271–280

Zhao G, Xu L, Xie L (2016) A simple and quantitative algorithm for identifying pulse-like ground motions based on zero velocity point method. Bull Seismol Soc Am 106(3):1011–1023